Reprint

Single Chip Controller for a High-Switching Frequency DC/AC Power Inverter

T. Antonakopoulos, S. Pressas and V. Makios

International Journal of Electronics

VOL. 73, NO. 1, 1992, pp. 229-240

INT. J. ELECTRONICS, 1992, VOL. 73, NO. 1. 229-240

Single chip controller for a high-switching frequency DC/AC power inverter

T. ANTONAKOPOULOS†, S. PRESSAS† and V. MAKIOS†

The design and implementation of a new controller for a DC/AC power inverter is described. The controller uses the high switching frequency sinusoidal PWM technique and achieves excellent output voltage regulation, frequency stability and dynamic response in a noiseless, light-weight and cost-effective construction. The inverter performance is analysed using experimental results as well as the harmonic analysis based on the generalized piecewise linear waveform representation. As these results indicate, most of the output power is concentrated on the fundamental harmonic component making the method suitable for use in driving inductive loads in various applications, such as photovoltaic systems.

1. Introduction

Pulse-width modulation (PWM) techniques are the techniques most commonly used to build inverters which generate AC output from fixed-voltage DC supply (Penalver *et al.* 1985). These PWM techniques compare a reference signal, a sinewave of desired frequency, to a modulating triangular wave of higher frequency. The process has been implemented using different hardware architectures, basically distinguished to analogue and digital or microcontroller-based (Buja and De Nardi 1985, Bowes and Clements 1982). The analogue architectures control the level of the inverter output continuously with negligible delay but they suffer from drift of the analogue components due to temperature variations and time. The microcontroller-based inverters are free from drift and disturbances, but their speed limitations are detrimental to the achievement of high control performance (Bowes and Clements 1982, Tzou and Wu 1988). To overcome these disadvantages, expensive and complicated signal processors have been used to generate the required triangle, the sinewave and finally the PWM signal (Buja and De Nardi 1985). The advantages gained by microcontroller methods are at the expense of more complex control, the cost of which reduces as the technology of chips and power semiconductor switches progresses.

Three distinct approaches have been used for PWM switching techniques: the natural sampling approach, the regular sampling approach and the optimal PWM approach (Buja and De Nardi 1985, Bowes and Clements 1982). The natural sampling approach is most widely used in analogue implementations, while the regular sampling approach has certain advantages when it is implemented in microcontroller-based systems. The optimized PWM switching technique is advantageous in low frequency ratios and is not of interest in this case.

For the analysis of the harmonic spectrum of the PWM waveforms, the Fourier series have been used in combination with the generalized piecewise linear waveform

Received 22 July 1991; revised 20 October 1991; accepted 4 November 1991.

†Laboratory of Electromagnetics, School of Engineering, University of Patras, 26500 Patras, Greece.

0020-7217/92 $3.00

representation (Bowes and Clements 1982). Using the results of the harmonic analysis, the inverter's designer can highlight the existing relations between the method's parameters and the harmonic characteristics, in order to modify them accordingly.

The implementation of a simple and computationally efficient PWM method is described here. The PWM method is the so-called high switching frequency sinusoidal and the inverter's control is implemented using only a single conventional microcontroller. In Section 2, the PWM switching technique is described and its advantages are highlighted. The implementation of the control section, the experimental results, and a short description of the various submodules of the inverter are discussed in Section 3. The harmonic analysis of the proposed PWM method is given and the theoretical results are compared to the experimental ones in Section 4. Section 5 summarizes the basic points and the results.

2. The high switching frequency sinusoidal PWM method

The operating principle used here, which is a type of regular sampled PWM, is called the high switching frequency sinusoidal PWM (HSFS-PWM). It is a combination of the low frequency sinusoidal PWM, used mainly on variable speed induction motor drives, and of the high frequency PWM, used on switching mode power supplies (Pressas and Makios 1989). The basic characteristics of this technique are the high switching frequency and the fixed position of the starting edge of each PWM pulse, as opposed to the fixed position of the centre of each PWM pulse usually used in symmetric regular sampled PWM methods.

Figure 1 shows the operating principle of the HSFS-PWM technique and Fig. 2 shows the pulse width determination. In order to pass from the analogue method to the digitally implemented technique, the so-called 'intersection-position determined' method was developed. Instead of a triangular carrier wave, a sawtooth wave is used

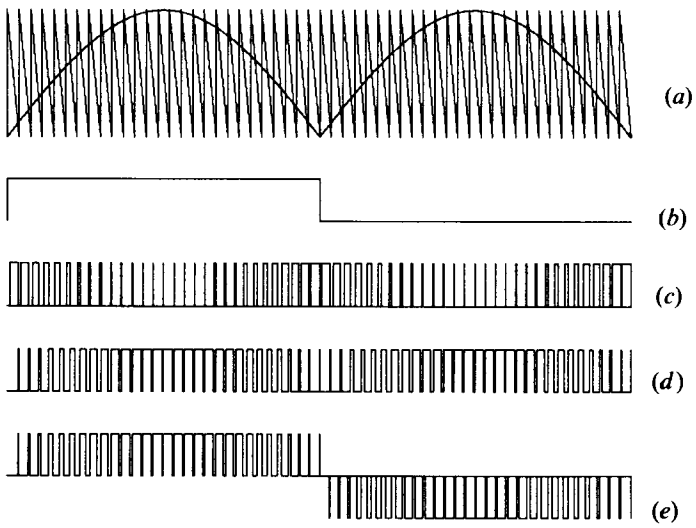

Figure 1. High switching frequency sinusoidal PWM method: (*a*) modulating and carrier signals; (*b*) polarity discriminator signal; (*c*) complementary PWM pulse train; (*d*) PWM pulse train; (*e*) equivalent 3-level PWM wave form.

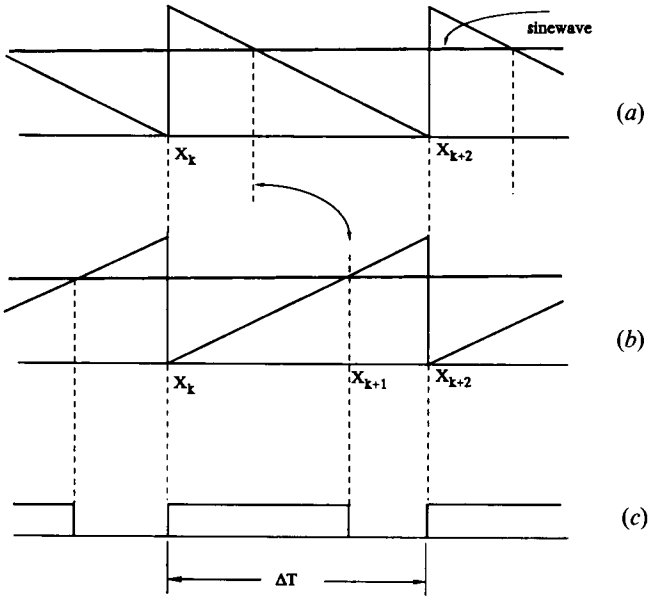

Figure 2. Details of the HSFS-PWM Method: (*a*) modulating and carrier signals; (*b*) 'intersection-position determined' method; (*c*) generated PWM pulse.

as the carrier signal, and the rising switching edge of the width-modulated pulse is determined by the intersection of the sinewave with the vertical edge of the reference signal (Fig. 2(*a*)). As a result, the start of each PWM pulse is at a fixed position. The position of the falling edge of the PWM pulse is determined by the value of the sine wave at the instant of the rising edge. This position can easily be determined using a symmetric sawtooth wave, as indicated in Fig. 2(*b*), by exploiting the symmetry of the two sawtooth waves and the fact that the sine wave can be considered to maintain the same level during each sawtooth interval. So the position of the falling edge of the PWM pulse is determined by the intersection of the sinewave with the symmetric sawtooth wave. This is a 'sample-and-hold' like operation which arises from the relation of the two signals and the fact that the used switching frequency ratio (carrier frequency/modulating frequency) is very high. The sawtooth method is considered ideal for analogue implementations of the HSFS-PWM technique, while the 'intersection-position determined' method is ideal for digital implementations. Because the pulse's position and duration are precisely defined, a programmable timer with a constant frequency clock can be used to determine the pulse position. For the determination of the pulse duration, a simple trigonometric function can be used or it can be extracted from a preloaded memory (like ROM). A digital implementation of this technique is described in detail in the next section.

It is well known that techniques of this type have the fundamental harmonic frequency equal to, and the amplitude proportional to the sine, while the remaining harmonics are placed in narrow bands centred around frequencies which are integer multiples of the carrier frequency. The higher the carrier frequency the less the smoothing action needed at the output of the inverter to obtain the sinusoidal waveform. Figure 1 shows this technique applied to a fully rectified sine wave and a

polarity discriminator has to be generated to form the output sine wave. Thus, it must be considered that the HSFS-PWM technique generates a 3-level waveform, which is typically used in line-to-line single-phase systems and this results in the elimination of carrier-frequency harmonics in the output sine wave.

3. The implemented controller

This controller has been used in a DC/AC power inverter for photovoltaic systems (Pressas and Makios 1989). The block diagram of the power inverter is shown in Fig. 3. The PWM pulses drive the power section through a totem-pole current boosting driving stage. Power MOSFETs have been used for the power switches connected in a push-pull configuration. The high frequency transformer is of a ferrite core type and its windings are made so as to avoid parasitic leakage inductances and interwinding capacitances. In order to avoid saturation problems, the inverter uses a symmetry correction circuit. The final stage of the inverter uses a bridge rectifier which consists of fast recovery diodes, a low-pass second-order L–C filter and an unfolding bridge which is commutated by the polarity discriminator signal of the control section. The nominal battery voltage is 48 V, the output voltage is pure sinusoidal 220 V(RMS)–50 Hz and the rated power is 1·5 kW. The inverter can supply AC power for heavily inductive loads and a path has been provided to return the reactive power to the battery. This inverter has excellent output voltage regulation and frequency stability, it is compact, noiseless and exhibits an excellent dynamic response.

The implementation of the high switching frequency sinusoidal PWM technique using digital (microcontroller-based) technology requires that the following functions be supported: (i) determination of the pulse position in constant length time intervals; (ii) determination of the pulse duration according to the phase of the generated sinewave; and (iii) calculation of the system response for feedback purposes.

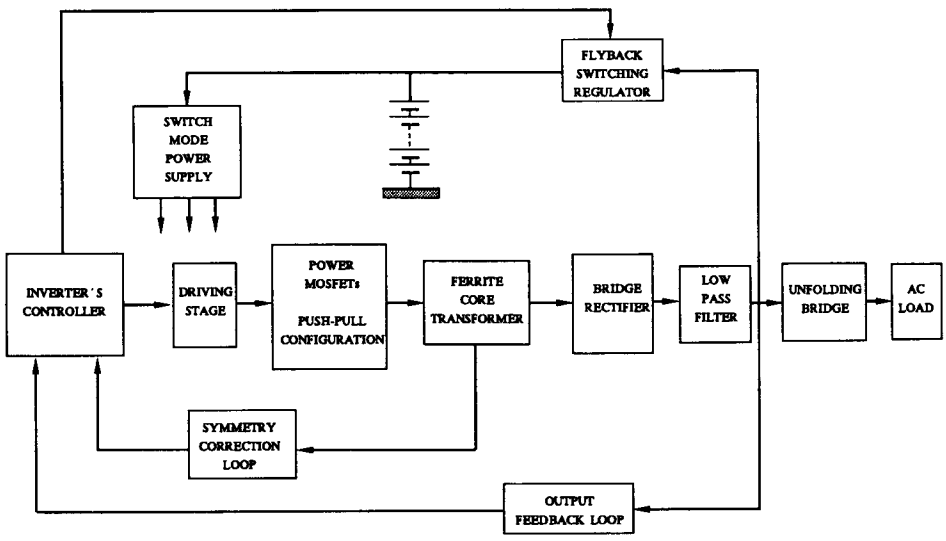

Figure 3. DC/AC power inverter block diagram.

In order to fulfil these requirements in a single chip configuration, the MC68HC11F1 microcontroller (Motorola Inc.) has been used. This microcontroller includes high resolution timing facilities, flexible and high-speed processing capabilities, analogue-to-digital converters, an interrupt-based structure and the appropriate amount of memory (RAM and electrically erasable PROM). It also has a 'computer operating properly (COP) watchdog system', which can be used for reliability purposes, while the included serial interface with the 'on-the-fly' EEPROM reprogramming capability can reduce the maintenance time of the controller to a few cycles of the generated sine wave.

The block diagram of the implemented controller is shown in Fig. 4. The controller uses two internal timers for PWM pulse generation and another timer for constant frequency pulse generation. Two timers are required for PWM pulse generation because the power switches are in a push-pull configuration and they must be driven by successive pulse alternately. The constant frequency pulses are generated for handling reactive power, as will be described later. The switching frequency of the implemented system is 16400 Hz while the frequency of the modulating sinewave is 50 Hz. The nominal speed of the microcontroller is 2 MHz (500 ns clock cycle) which will be increased to 4 MHz as the new version becomes available. Using the new version of the MC68HC11F1, the switching frequency can be increased to 33 kHz without any modifications to the stored program (only the stored look-up table has to be updated). At these speeds, the only limitations are the switching capabilities of the used power semiconductor switches. The controller can generate the sine wave in a straightforward format, when no line sensing is required, but it can also use feedback data in a carrier-cycle step to take into account the line's status in the sine wave generation. After the system initialization, constant length routines are used to determine the position of the starting edge of each PWM pulse. The duration of each PWM pulse is stored in the internal ROM and a look-up table is formed. The microcontroller has an internal free-running counter with 500 ns resolution and the PWM timers are driven by this clock. Thus, the stored pulse duration values determine the number of clock cycles, that the timer has to count, to define the respective duration.

In simple, no feedback operation, the CPU core (Fig. 3) scans this look-up table and feeds the two timers alternately to generate the PWM pulses. In the normal system operation, the output voltage is sensed and is fed to the A/D channel in a rectified form. The CPU core translates the received value to PWM pulse duration

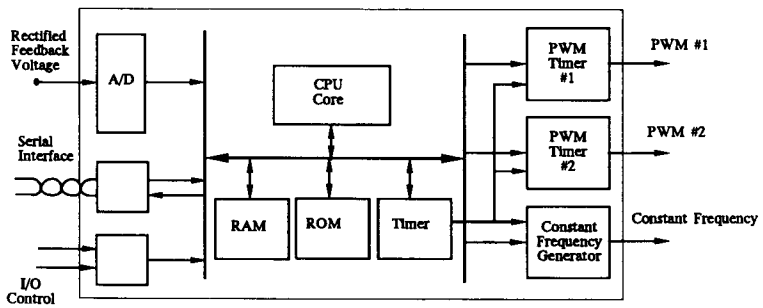

Figure 4. Block diagram of controller.

form and subtracts this value from the value used k-steps previously. (A step is assumed to be the time between the starting edges of two successive PWM pulses. The duration of the k-steps is equal to the system's total lag which is mainly determined by the output filter. The value of 'k' is adjusted to minimize the output sine wave distortion.) The result of the subtraction is added algebraically to the current look-up table value and is fed to the appropriate PWM timer. Figure 5 shows the block diagram of the internal processing procedure. In order to minimize the required processing, instead of the ideal PWM durations, the EEPROM contains the sum of two ideal patterns, one of which is shifted in a cyclic form with k-positions. This implies that in each PWM generation only a subtraction is required, allowing a great number of pulses to be generated in each sine wave period. The maximum length of the PWM pulses is equal to the interpulse duration minus 1 μs, to prevent the power semiconductor switches from short-circuit ('shoot-through'), due to different turn-on and turn-off switching times (Varnovitsky 1984). Figure 6 shows the two PWM output pulse trains, the polarity discriminator signal, the 'folded' sine wave and the generated sine wave. The experimental results were obtained using ohmic load, thus the current and voltage waveforms are similar. In the following diagrams, the voltage waveform is indicated. Figure 7 shows the experimental harmonic spectrum of the sinewave. The overall harmonic contents are clearly low: the power of the fundamental harmonic is 30 db greater than the next harmonic and almost the total power of the output sine wave is concentrated on the fundamental harmonic. A small percentage of the total power is concentrated in the harmonics around the frequency of the carrier signal and so it must be considered negligible. Higher harmonics are less significant. A more detailed discussion is given below in relation to a theoretical harmonic analysis.

When driving inductive loads, the controller must handle reactive power by providing a path to the battery. This is achieved by sensing a regeneration interval using the I/O control section. The duration (t_{reg}) of the regeneration interval is defined by:

$$t_{reg}=\frac{1}{\omega}\tan^{-1}\left(\frac{\omega L}{R}\right)$$

where R and L are the resistive and inductive components of the system's load, respectively. After detecting the start of that interval, the PWM timers are stopped and a constant frequency generation is started. During this interval, the reactive

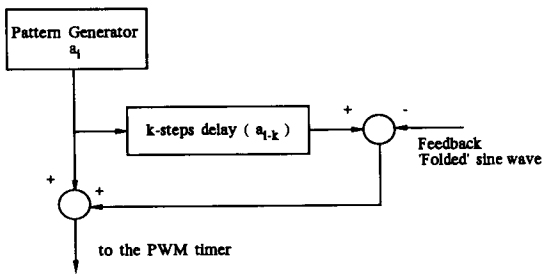

Figure 5. Internal processing operation.

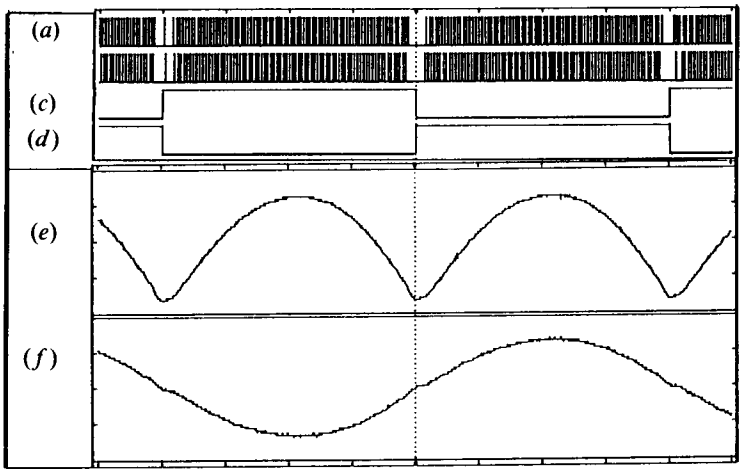

Figure 6. Sine wave generation process: (*a*) output of the PWM no. 1 timer; (*b*) output of the PWM no. 2 timer; (*c*) polarity discriminator signal; (*d*) complementary polarity discriminator signal; (*e*) 'folded' sine wave; (*f*) output sine wave (voltage: 220 V R.M.S.).

power generated on the load is fed back to the system battery under the control of the new generated signal. When the generation interval terminates, the controller continues its PWM function, not from the point where it had been stopped but from the point where it should have been if there was no regeneration interval. Figure 8 shows the inverter output during a regeneration interval and details of the regeneration process.

4. Harmonic analysis

It has been found that the content of the harmonic components produced by the inverter is the fundamental characteristic of the used modulation strategy. The generated output must have its power concentrated on the fundamental component

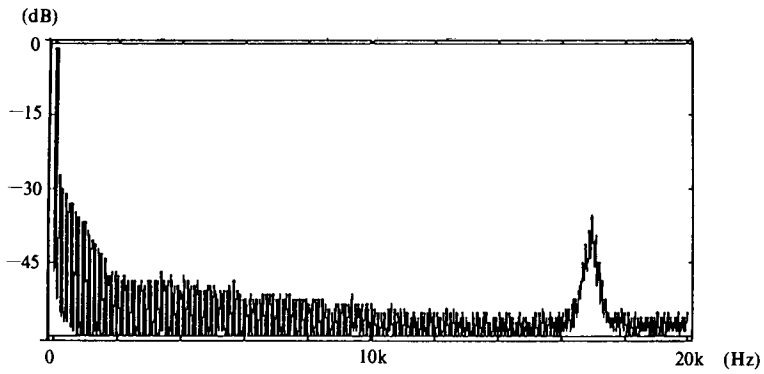

Figure 7. Experimental harmonic spectrum.

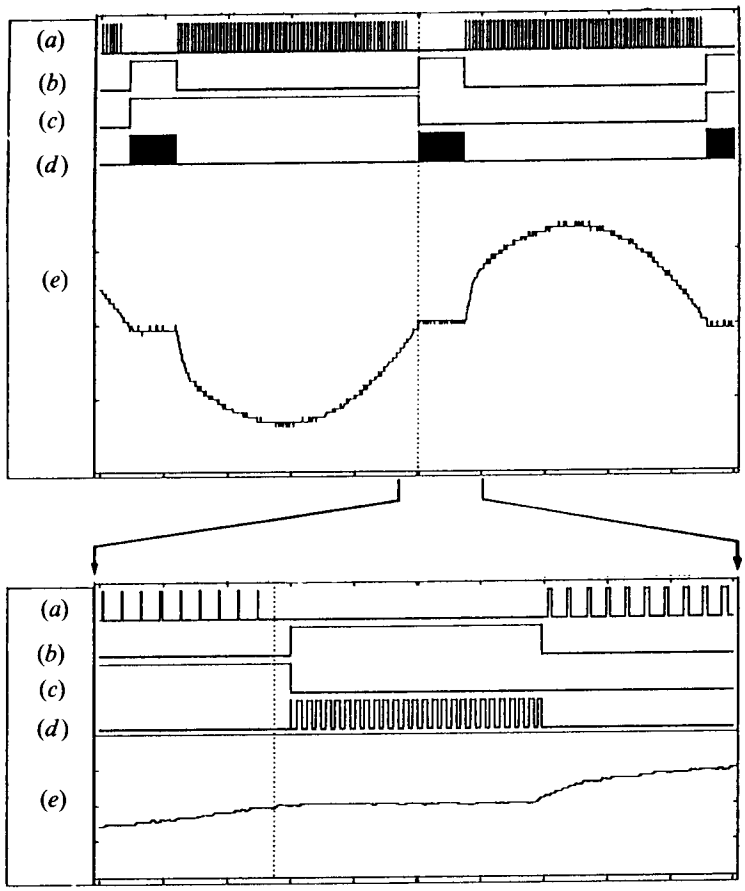

Figure 8. Inverter regeneration process: (*a*) PWM signal; (*b*) constant frequency signal; (*c*) polarity discriminator signal; (*d*) regeneration phase indicator; (*e*) output sine wave (voltage: 220 V R.M.S.).

and the higher-order harmonics must be minimized, while no DC component should exist. In order to derive the harmonic analysis of the previously described technique, the generalized piecewise linear waveform representation is used (Tzou and Wu 1988). From the Fourier series analysis, it is known that a half-cycle symmetric periodic function, such as the used PWM pulse train, consists only of odd harmonic terms. The switching function, $S(\omega t)$, of the used PWM modulation can be defined as:

$$S(\omega t) = A_0 + \sum_{n=1}^{\infty} (A_n \cos(n\omega t) + B_n \sin(n\omega t)) \tag{1}$$

The harmonic analysis of the PWM output is achieved by determining the Fourier coefficients of (1). In Fig. 9(*a*), an interval of the general piecewise linear waveform is shown and will be used as the basic unit for the PWM representation, as shown in Fig. 9(*b*). The output PWM pulse train is a piecewise linear periodic

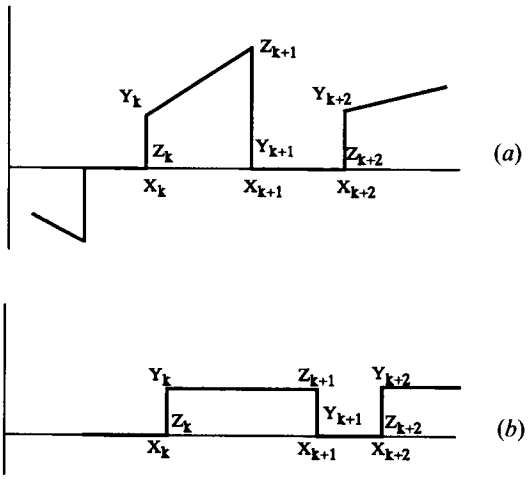

Figure 9. Piecewise linear waveform presentation and its application to a PWM pulse train (Tzou and Wu 1988).

waveform, which contains two types of constant height pieces and variable length subintervals. The first type of interval has a length proportional to the current value of the ideal sine and a height which is equal to one while the second type of intervals has zero height and length equal to the distance of the rising edge of two successive pulses minus the length of the last first-type interval.

Bearing in mind:

(i) The modulation depth which is the ratio of the amplitude of the reference sine wave to the amplitude of the sawtooth, is $M=1$.
(ii) There are N PWM pulses in each period of the output sine, thus there are $2N$ piecewise intervals.
(iii) The distance between two successive pulses, ΔT, is constant and equal to $2\pi/N$ radians of the generated sine.

the Fourier coefficients are given as:

$$A_0=\frac{1}{2\pi}\cdot\sum_{\substack{k=1\\ inc2}}^{2N-1}(X_{k+1}-X_k)\cdot V(k) \tag{2}$$

$$A_n=\frac{1}{n\pi}\cdot\sum_{\substack{k=1\\ inc2}}^{2N-1}[\sin(nX_{k+1})-\sin(nX_k)]\cdot V(k) \tag{3}$$

$$B_n=\frac{1}{n\pi}\cdot\sum_{\substack{k=1\\ inc2}}^{2N-1}[\cos(nX_k)-\cos(nX_{k+1})]\cdot V(k) \tag{4}$$

where $V(k)$ is equal to 1 for the first half period and -1 for the second half period, and

$$X_{k+1}-X_k=\Delta T\cdot M\left|\sin\left(\frac{\pi}{N}(k-1)\right)\right| \tag{5}$$

Using the following equations:

$$X_k=\frac{\pi(k-1)}{N} \tag{6}$$

$$X_{k+1}=\frac{\pi(k-1)}{N}+\frac{2M\pi}{N}\left|\sin\left(\frac{\pi(k-1)}{N}\right)\right| \tag{7}$$

$$\sum_{\substack{k=1\\ inc2}}^{\frac{N}{2}-1}\sin(nX_k)=\frac{[1-\cos(n\pi)]}{2}\frac{\cos\left(\frac{n\pi}{N}\right)}{\sin\left(\frac{n\pi}{N}\right)} \tag{8}$$

$$\sum_{\substack{k=1\\ inc2}}^{\frac{N}{2}-1}\cos(nX_k)=\frac{[1-\cos(n\pi)]}{2} \tag{9}$$

it can be easily proved that the Fourier coefficients are given by:

$$A_0=0 \tag{10}$$

$$A_n=\frac{[1-\cos(n\pi)}{2}\left[\sum_{k=1}^{\frac{N}{2}-1}\left(\sin\left(\frac{2\pi nk}{N}+\frac{2\pi nM}{N}\left|\sin\left(\frac{2\pi k}{N}\right)\right|\right)\right)-\frac{[1-\cos(n\pi)]}{2}\frac{\cos\left(\frac{n\pi}{N}\right)}{\sin\left(\frac{n\pi}{N}\right)}\right] \tag{11}$$

$$B_n=\frac{[1-\cos(n\pi)]}{2}\left[\frac{[1-\cos(n\pi)]}{2}-\sum_{k=0}^{\frac{N}{2}-1}\left(\cos\left(\frac{2\pi nk}{N}+\frac{2\pi nM}{N}\left|\sin\left(\frac{2\pi k}{N}\right)\right|\right)\right)\right] \tag{12}$$

From these equations, it is obvious that no DC component exists in the generated output and there are no even harmonics. Applying the implementation parameters to these equations, the harmonic analysis diagram is derived. Figure 10 shows the power distribution in the various frequency harmonics. The power of the fundamental harmonic is used as the reference value and for each harmonic component the $10\log(P_i/P_1)$ is given, where P_i is the power of the ith harmonic. The fundamental component (50 Hz) contains 84·775% of the total power, the harmonics around the carrier frequency contain about 11·6% of the total power, while 3·4% of the total power is contained in the vicinity of the second harmonic of the carrier frequency. The Table indicates the values of the theoretical and the experimental relative power distribution in various harmonics. The differences between the theoretical and the experimental values occur because the power section of the inverter acts as a low-pass filter and that results in the attenuation of the high

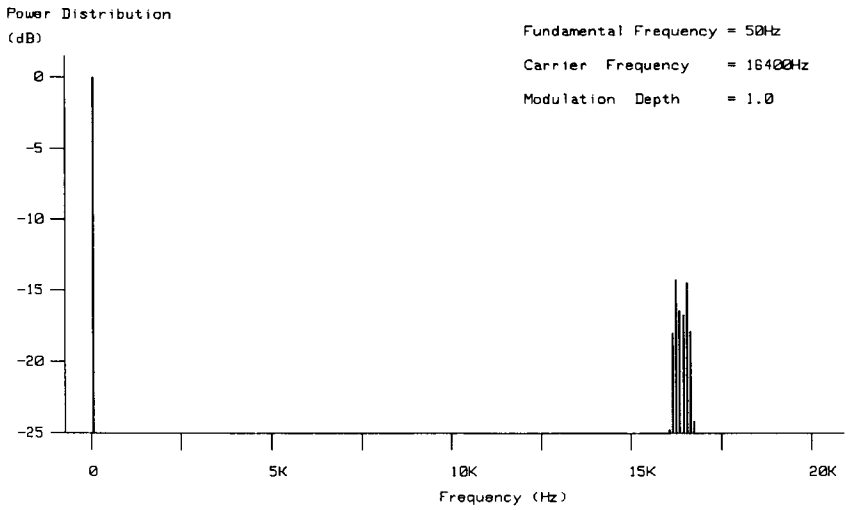

Figure 10. Harmonic analysis of HSFS-PWM method.

frequency components. This explains the differences of the relative power distribution in the area of 16 400 Hz (the carrier frequency).

In the area of the low-order harmonics, the differences are due to the quantization errors which are inherent in the digital systems due to the finite number of discrete PWM lengths (which was not taken into account in the previously described mathematical analysis).

Generally, it can be said that the theoretical results are in conformity with the experimental ones presented in Fig. 7. The concentration of the output power to the fundamental component implies that small power filters must be used in the DC/AC

Frequency (Hz)	Relative power (theoretical) (dB)	Relative power (experimental) (dB)
50	0	0
150	−46·2	−34·2
250	−58·7	−37·0
350	−65·3	−41·8
450	−69·9	−43·4
550	−73·6	−45·7
16150	−18·0	−63·2
16250	−14·2	−56·1
16350	−16·5	−52·6
16450	−14·5	−48·9
16550	−17.9	−55·1
16650	−24·2	−61·8

Relative power distribution in various harmonics of the HSFS-PWM method (carrier frequency = 16 400 Hz, modulating frequency = 50 Hz).

inverter and that a small percentage of the generated energy will be consumed by these filters.

5. Conclusions

A single chip implementation of the control unit of a high-switching frequency DC/AC inverter has been presented. The high switching frequency sinusoidal PWM technique has been used while the controller has been implemented using a conventional microcontroller. Various facilities have been included to increase the system reliability. Feedback control of the output sine wave is also used to improve the system's performance. The experimental results show the system's performance and highlight the advantages offered by the switching technique used. The system's performance is also presented through the use of a piecewise linear waveform representation for the Fourier series analysis. The theoretical results are in conformity with the experimental results, which prove that the technique used is ideal in providing pure sinusoidal output for applications such as photovoltaic systems driving inductive loads.

Acknowledgment

The authors wish to thank Mr C. Papadopoulos for his assistance during the implementation of the prototype.

References

Bowes, S. R., and Clements, R. R., 1982, Computer-aided design of PWM inverter systems. *Proceedings of the Institution of Electrical Engineers*, Pt B, **129,** 1-17.

Buja, G. S., and De Nardi, P., 1985, Application of a signal processor in PWM inverter control. *I.E.E.E. Transactions on Industrial Electronics*, **32,** 50-55.

Penalver, C. M., Peire, J., and Martinez, P. M., 1985, Microprocessor control of DC/AC static converters. *I.E.E.E. Transactions on Industrial Electronics*, **32,** 186-191.

Pressas, S., and Makios, V., 1989, A light weight, four quadrant, high switching frequency modular photovoltaic DC/AC inverter with sinusoidal output and high efficiency. *20th I.E.E.E. Photovoltaic Specialists Conference*, Las Vegas.

Tzou, Y. Y., and Wu, Y. C., 1988, Harmonic analysis of PWM inverter modulation strategies. *International Journal of Electronics*, **64,** 461-480.

Varnovitsky, M., 1984, Development and comparative analysis of a pulse-width modulation strategy. *I.E.E.E. Transactions on Industrial Electronics*, **31,** 272-276.